OPEN ACCESS Freely available online

PLOS ONE

Friction in Total Hip Joint Prosthesis Measured *In Vivo* during Walking

Philipp Damm[1]*, Joern Dymke[1], Robert Ackermann[1], Alwina Bender[1], Friedmar Graichen[1], Andreas Halder[2], Alexander Beier[2], Georg Bergmann[1]

1 Julius Wolff Institute, Charité – Universitaetsmedizin Berlin, Berlin, Germany, **2** Klinik für Endoprothetik, Sana Kliniken Sommerfeld, Sommerfeld, Germany

Abstract

Friction-induced moments and subsequent cup loosening can be the reason for total hip joint replacement failure. The aim of this study was to measure the *in vivo* contact forces and friction moments during walking. Instrumented hip implants with Al_2O_3 ceramic head and an XPE inlay were used. *In vivo* measurements were taken 3 months post operatively in 8 subjects. The coefficient of friction was calculated in 3D throughout the whole gait cycle, and average values of the friction-induced power dissipation in the joint were determined. On average, peak contact forces of 248% of the bodyweight and peak friction moments of 0.26% bodyweight times meter were determined. However, contact forces and friction moments varied greatly between individuals. The friction moment increased during the extension phase of the joint. The average coefficient of friction also increased during this period, from 0.04 (0.03 to 0.06) at contralateral toe off to 0.06 (0.04 to 0.08) at contralateral heel strike. During the flexion phase, the coefficient of friction increased further to 0.14 (0.09 to 0.23) at toe off. The average friction-induced power throughout the whole gait cycle was 2.3 W (1.4 W to 3.8 W). Although more parameters than only the synovia determine the friction, the wide ranges of friction coefficients and power dissipation indicate that the lubricating properties of synovia are individually very different. However, such differences may also exist in natural joints and may influence the progression of arthrosis. Furthermore, subjects with very high power dissipation may be at risk of thermally induced implant loosening. The large increase of the friction coefficient during each step could be caused by the synovia being squeezed out under load.

Citation: Damm P, Dymke J, Ackermann R, Bender A, Graichen F, et al. (2013) Friction in Total Hip Joint Prosthesis Measured *In Vivo* during Walking. PLoS ONE 8(11): e78373. doi:10.1371/journal.pone.0078373

Editor: Amir A. Zadpoor, Delft University of Technology (TUDelft), The Netherlands

Received May 21, 2013; **Accepted** September 20, 2013; **Published** November 8, 2013

Funding: Funding provided by the German Research Society (SFB760 and BE 804/19-1), http://www.dfg.de, and Deutsche Arthrose-Hilfe e. V., http://www.arthrose.de. The funders had no role in study design, data collection and analysis, decision to publish, or preparation of the manuscript.

Competing Interests: The authors have declared that no competing interests exist.

* E-mail: Philipp.Damm@charite.de

Introduction

In 20% to 40% of all cases [1], polyethylene wear and aseptic loosening are the most frequent reasons for revisions of total hip joint replacements (THR). Both factors are related to friction in the joint. Cup loosening has been reported to be the only cause in 30% to 62% of revisions [2,3]. Subjects, who obtained a THR are becoming increasingly younger and are, therefore, more active and athletic [4,5]. However, higher activity levels produce more wear and more strenuous activities cause higher friction moments. This will increase the risk of implant loosening [6,7]. These facts indicate that reduction of friction between head and cup is critical for further improvement of THR.

Several *in vivo* studies have been performed to investigate the loads acting in hip implants during different activities [8,9]. These studies have shown that the contact force during normal walking falls in a range between 240 and 480% of the bodyweight (BW). However, *in vivo* measurements of friction in hip endoprostheses have not been reported previously.

One *in vivo* study *indirectly* assessed friction in the joint by measuring the implant temperature during an hour of walking [10,11]. Its increase is mainly related to the friction-induced power generated in the implant. A peak temperature of 43.1°C was measured in 1 subject, a level at which bone tissue may already be impaired [12], especially when this temperature occurs repeatedly. Therefore, it cannot be excluded that friction and increased implant temperatures may be underestimated risk factors for the long-term stability of THR.

To determine the friction in total hip joint prosthesis, *in vitro* simulator studies were performed [13,14]. To evaluate the friction between two sliding partners, the coefficient of friction μ was used. For the tribological pairing Al_2O_3/UHMWPE μ ranges depended on the lubricant [13], ranging from 0.044 (distilled water), to 0.054 (bovine serum), and 0.089 (saline). The coefficient increased dramatically up to values of 0.14 when the conditions changed from lubricated to dry [15].

However, most of the simulator tests load the joint only in the flexion-extension plane and use load patterns which may not be realistic [16]. Newer studies investigated friction under more realistic conditions, simulating *in vivo* measured gait data [17]. Varying parameters for friction were investigated, for example, different material combinations for implant head and cup [18], and various lubricant regimes [17,19–22]. These simulator studies were performed under very different test conditions, such as deviating patterns of joint loading and movement or by using different lubricants. Nevertheless, it was shown that friction in THR is mainly influenced by the material of the sliding partners and the lubrication regime.

Table 1. Patients investigated.

Patient	Age	Gender	Body weight	Gait Velocity	Mean Gliding Speed Extension | Flexion
	[years]		[N]	[m/s]	[m/s]
H1	56	m	754	1.0	0.02 | 0.04
H2	62	m	755	1.0	0.03 | 0.05
H3	60	m	880	0.8	0.02 | 0.06
H4	50	m	783	1.0	0.03 | 0.06
H5	62	f	853	0.9	0.02 | 0.08
H6	69	m	832	1.1	0.03 | 0.05
H7	53	m	899	1.1	0.03 | 0.06
H8	56	m	779	1.1	0.03 | 0.06
Average	*59*	-	*821*	*1.0*	*0.03 | 0.06*

doi:10.1371/journal.pone.0078373.t001

The aim of our study was to determine the *in vivo* contact forces in hip implants during walking, plus the moments caused by friction, and derive the coefficient of friction from these data. These data will help to understand the *in vivo* lubrication conditions and allow validating, potentially improving the conditions applied in joint simulators.

Methods

Ethic statement

The study was approved by the Charité Ethics committee (EA2/057/09) and registered at the 'German Clinical Trials Register' (DRKS00000563). All patients gave written informed consent prior to participating in this study.

Subjects and measurements

Eight subjects with instrumented hip joint prostheses (Table 1) participate in this study. Measurements were taken 3 months postoperatively (pOP) during level walking at a self-selected walking speed. Selected trials of each investigated subject are also shown and can be downloaded at the public data base www.OrthoLoad.com.

Measuring equipment

Joint forces and friction moments were measured *in vivo* with instrumented hip implants. The prosthesis (CTW, Merete Medical, Berlin, Germany) has a titanium stem, a 32 mm Al_2O_3 ceramic head (BIOLOX forte, CeramTec GmbH, Plochingen, Germany) and an XPE inlay (Durasul, Zimmer GmbH, Winterthur, Switzerland). A telemetry circuit, 6 strain gauges, and a secondary induction coil are placed in the hollow neck, which is closed by welding. A detailed description of the instrumented implant was published previously [23]. A coil around the hip joint inductively powers the inner electronics. The strain gauge signals are transferred via an antenna in the implant head to the external receiver. These signals and the subject's movements are recorded simultaneously on videotape. The external measurement system has previously been described in detail [24,25].

From the 6 strain gauge signals, the 3 force and 3 moment components acting on the implant head are calculated [26] with an accuracy of 1–2%. The femur-based coordinate system [27] is fixed in the center of the head of a right sided implant, but is defined relative to the bone. Data from left implants were mirrored to the right side. The positive force components F_x, F_y, and F_z act in lateral, anterior, and superior directions, respectively (Figure 1A). From the 3 force components the resultant contact force F_{res} is calculated. The measured friction moments M_x, M_y, and M_z, act clockwise around the positive axes. The 3 moment components deliver the resultant friction moment M_{res}. Positive/negative moments M_x are caused by extension/flexion of the joint. Positive/negative moments M_y act during abduction/adduction. Positive/negative moments M_z are caused by external/internal rotation.

Data evaluation

All forces are reported as percent of bodyweight (% BW) and the friction moments as % BWm. Average force-time patterns

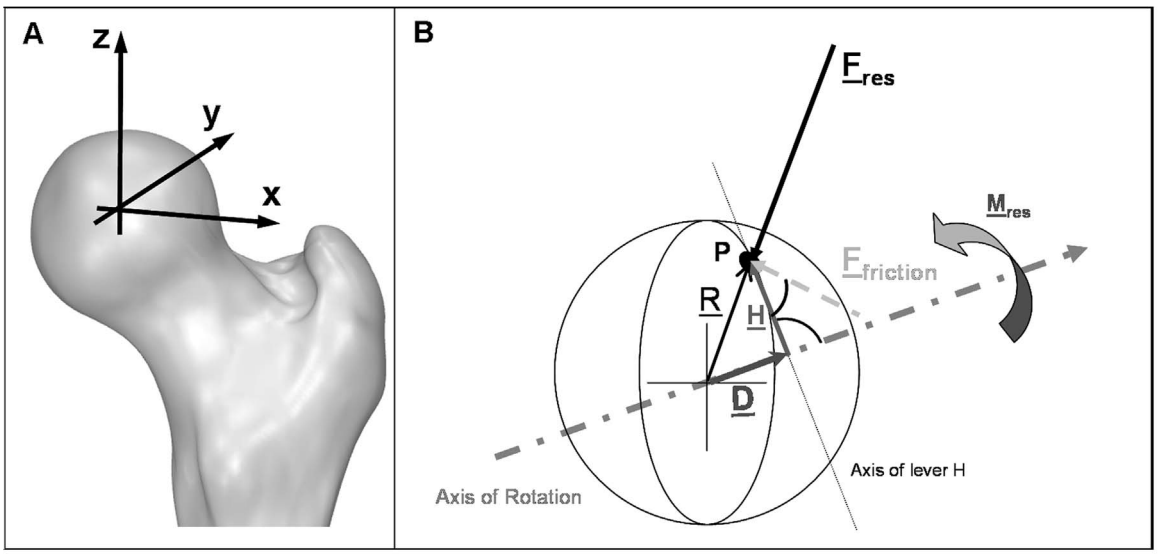

Figure 1. Coordinate system and vectors for calculation of the coefficient of friction μ. Right joint, posterior view.
doi:10.1371/journal.pone.0078373.g001

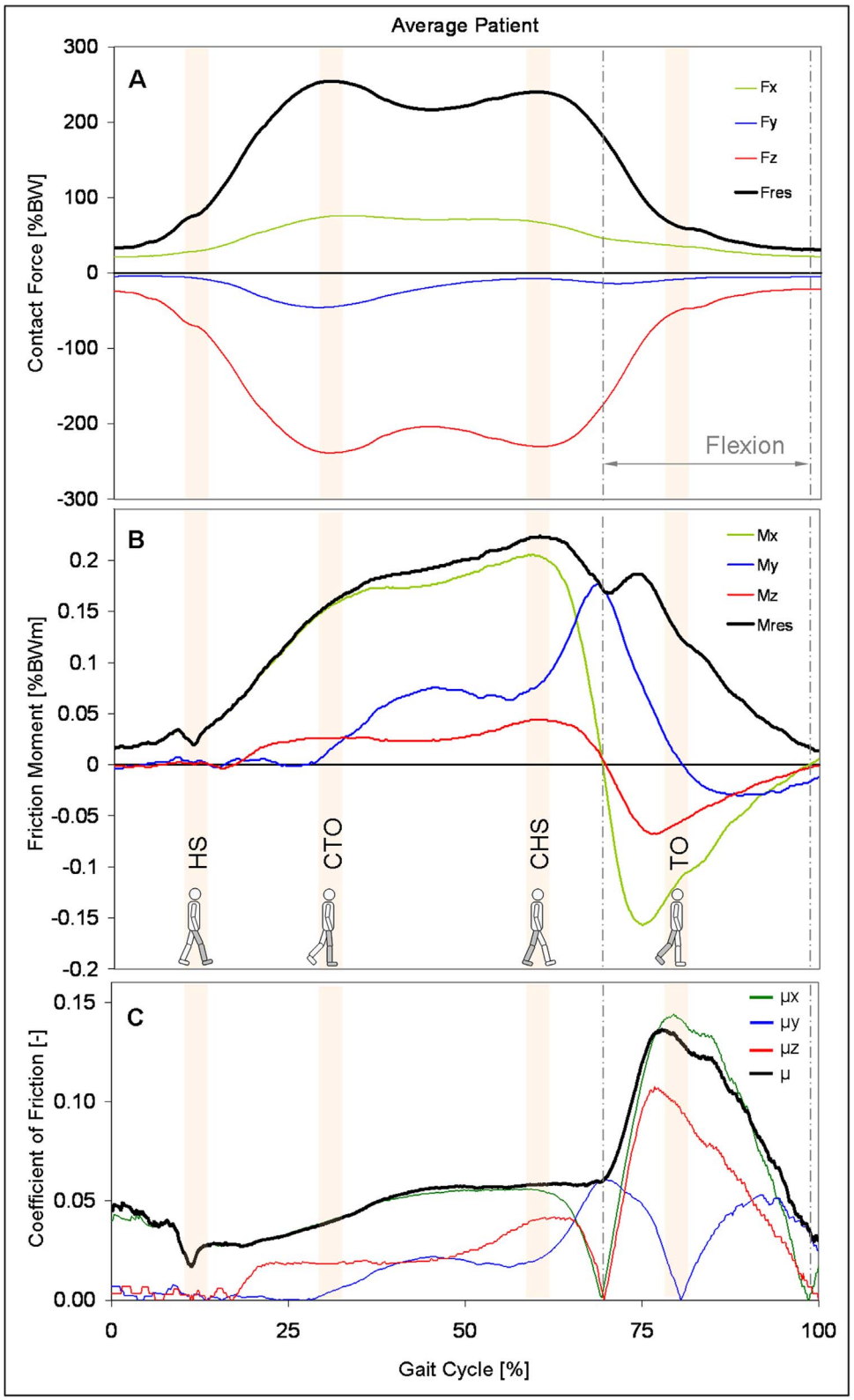

Figure 2. Time courses of contact force, friction moment, and coefficient of friction. Top: contact force F_{res} and its components. Middle: friction moment M_{res} and its components. Bottom: coefficients of friction.μ from 3D calculation; μ_x (sagittal plane), μ_y (frontal plane), and μ_z (horizontal plane) from simplified 2D calculations. The data presented are for an average subject during level walking at approximately 1 m/s. Vertical lines: borders of the flexion phase. The diagram starts before heel strike.
doi:10.1371/journal.pone.0078373.g002

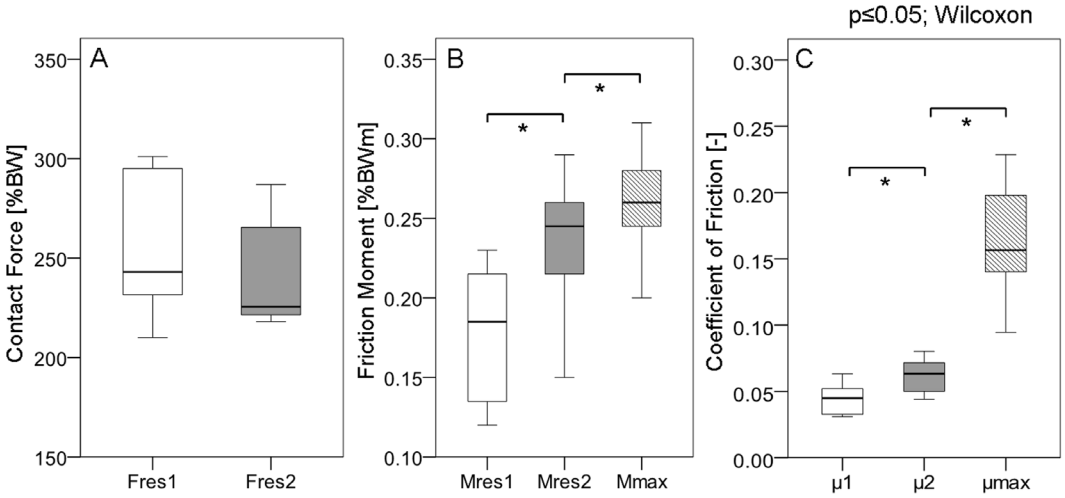

Figure 3. Peak values of contact force, friction moment and coefficient of friction. A: contact force F_{res}, B: friction moment M_{res}, C: coefficient of friction μ. Individual numerical mean values and ranges from 8 subjects. $M_{res1}|M_{res2}$, $\mu_1|\mu_2$ = values at the instant of the force maxima $F_{res1}|F_{res2}$ (see Figure 2). M_{max}, μ_{max} = absolute maxima during a whole walking cycle.
doi:10.1371/journal.pone.0078373.g003

from 32–96 steps were calculated for each subject. The employed 'time warping' method [28] weighted the congruency of high forces more than that of lower ones. First the period times of all the included steps are normalized. The single time scales were then distorted in such a way that the squared differences between all deformed curves, summed over the whole cycle time, were smallest. Finally, an arithmetically averaged load-time pattern was calculated from all the deformed curves. Using these algorithms, an average time course was first calculated from the time patterns of the resultant joint forces F_{res}. The obtained time deformations of the single trials were then transferred to the corresponding force and moment components before averaging them, too. The resultant friction moment M_{res} was calculated from an average of its components.

This procedure was first applied on all trials of the single subjects, leading to 'individual' averages. These averages from all subjects were then combined to a 'general' average, which describes the loads acting in an 'average' subject.

In some cases, peak values were not taken from the averaged time courses, but instead, the numerical peak values of the *single* trials were averaged, first individually and then inter-individually. Extreme values of the averaged load-time patterns can slightly deviate from these numerically averaged numbers. These values of the average subject were statistically analysed ($p \leq 0.05$; Wilcoxon).

Coefficient of friction

The coefficient of friction μ between the head and the cup was calculated by a 3D approach (Figure 1B). Joint movement takes place in a plane perpendicular to the axis of the vector $\underline{M}_{res}$. This axis is not perpendicular to the axis of vector $\underline{F}_{res}$. The vector of the friction force $\underline{F}_{friction}$ acts perpendicular to $\underline{F}_{res}$ at point P on the head. $\underline{H}$ is the vector of the lever arm between $\underline{F}_{Friction}$ and the axis of $\underline{M}_{res}$ and is perpendicular to both. $\underline{D}$ is a vector in direction of $\underline{M}_{res}$. $\underline{R} = 16$ mm is the radius vector to point P.

Assuming a Coulomb friction between the head and the cup, the friction force acting on the head is

$$F_{friction} = \mu * F_{res} \quad (1)$$

The moment determined by the force $\underline{F}_{friction}$ and its lever arm $\underline{H}$ has to counteract $\underline{M}_{res}$. Because $\underline{F}_{friction}$ and $\underline{H}$ are perpendicular to each other, this delivers the scalar equation

$$H * F_{friction} = M_{res} \quad (2)$$

From the combination of (1) and (2), the following equation can be derived:

$$\mu = M_{res}/(H * F_{res}) \quad (3)$$

$\underline{R}$ is the radius of the head. R points to P and has the direction opposite to $\underline{F}_{res}$:

$$\underline{R} = -R * \underline{F}_{res}/F_{res} \quad (4)$$

$\underline{H}$ can be substituted by

$$\underline{H} = \underline{R} - \underline{D} \quad (5)$$

With $\underline{D}$ being the orthogonal projection of $\underline{R}$ on $\underline{M}_{res}$:

$$\underline{D} = R * \cos(\underline{R},\underline{M}_{res}) * \underline{M}_{res}/M_{res} \quad (6)$$

The angle between $\underline{R}$ and $\underline{M}_{res}$ can be derived from their scalar product:

$$\cos(\underline{R},\underline{M}_{res}) = (\underline{R} * \underline{M}_{res})/(R * M_{res}) \quad (7)$$

Applying (4), (6), (7), equation (5) becomes

$$\underline{H} = R * (\underline{F}_{res}/F_{res}) * [(\underline{M}_{res}/M_{res})^2 - 1] \quad (8)$$

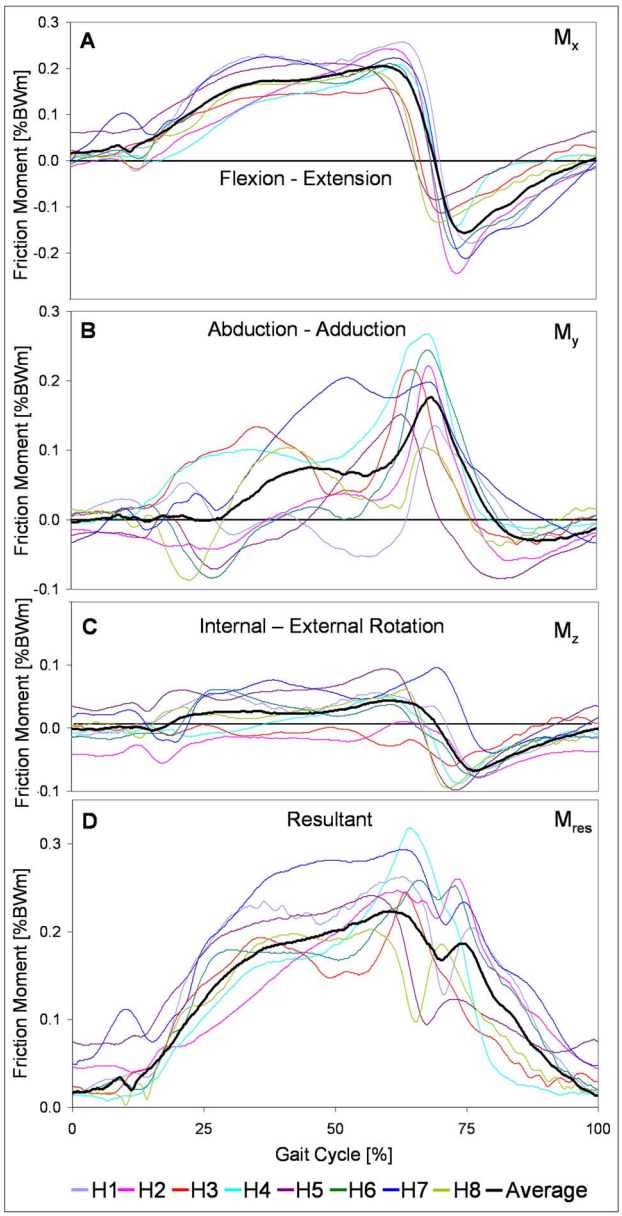

Figure 4. Components of friction moment. Components M_x, M_y, M_z around x, y, z axes (see Figure 1). Individually averaged patterns of subjects H1 to H8 (color), and average patterns of all subjects (black).
doi:10.1371/journal.pone.0078373.g004

The friction coefficient μ is determined from (3), using the measured load vectors $\underline{F}_{res}$ and $\underline{M}_{res}$, the known head radius R, and the lever arm H, which is calculated by (8). Due to measuring errors, μ will be inaccurate if $\underline{F}_{res}$ or $\underline{M}_{res}$ is very small. Therefore, μ was only determined for $F_{res} \geq 20\%$ BW *and* $M_{res} \geq 0.02\%$ BWm.

In previous simulator tests, μ has mostly been determined in the sagittal plane. To compare our 3D-derived values with this data, we additionally calculated μ from the forces and moments measured in the sagittal, frontal, and horizontal planes as follows:

$$\mu_x = M_x/(F_{yz} * R) \quad (9a)$$

$$\mu_y = M_y/(F_{xz} * R) \quad (9b)$$

$$\mu_z = M_z/(F_{xy} * R) \quad (9c)$$

F_{yz}, F_{xz} and F_{xy} are the forces in the sagittal, frontal, and horizontal planes, respectively.

Friction-induced power

In addition to the measured joint loads and the calculated friction coefficient μ, we determined the friction-induced power Q in the joint, which is caused by the friction force $F_{friction}$. With v being the gliding speed between head and cup, Q is given by the simplified equation

$$Q = F_{friction} * v = F_{res} * \mu * v \quad (10)$$

Average values of Q were calculated separately for the extension and flexion phases of the gait cycle:

$$Q_{ext} = F_{ext} * \mu_{ext} * v_{ext} \quad (11a)$$

$$Q_{flex} = F_{flex} * \mu_{flex} * v_{flex} \quad (11b)$$

The average power Q_{aver} over the *whole* gait cycle was then determined from

$$Q_{aver} = (Q_{ext} * T_{ext} + Q_{flex} * T_{flex})/(T_{ext} + T_{flex}) \quad (11c)$$

Calculations were based on the intra-individually averaged load-time patterns of the single subjects. Before F_{ext}, μ_{ext}, F_{flex}, and μ_{flex} were inserted in (11a, b), their time-dependent values were averaged arithmetically over the corresponding time periods T_{ext} and T_{flex}. The speed v was determined from the flexion/extension range of the shank in the sagittal plane, the times of flexion and extension, and the radius of the prosthetic head. The data of 4–7 steps per subject were averaged. Because no gait analyses had been performed, the shank movement had to be determined from the patient videos. The Intra-observer variation of v and therefore Q was on average 1%, the inter-observer variability of four investigators was on average 2%.

Results

Unless stated otherwise, the values reported here were taken from the time patterns of the average subject. The notation "X|Y" indicates a value of X at the instant of the first peak F_{res1} of the resultant force and a value of Y at the second peak F_{res2}.

Joint contact forces

Figure 2A shows the time patterns of F_{res} and its components for the average subject during one walking cycle. F_{res} was nearly identical with $-F_z$; the latter acts distally along the z-axis of the femur and compresses the hip joint. F_{res} had 2 peak values $F_{res1}|F_{res2}$. F_{res1} acted at about the time of contralateral toe off (CTO) and F_{res2} close to contralateral heel strike (CHS).

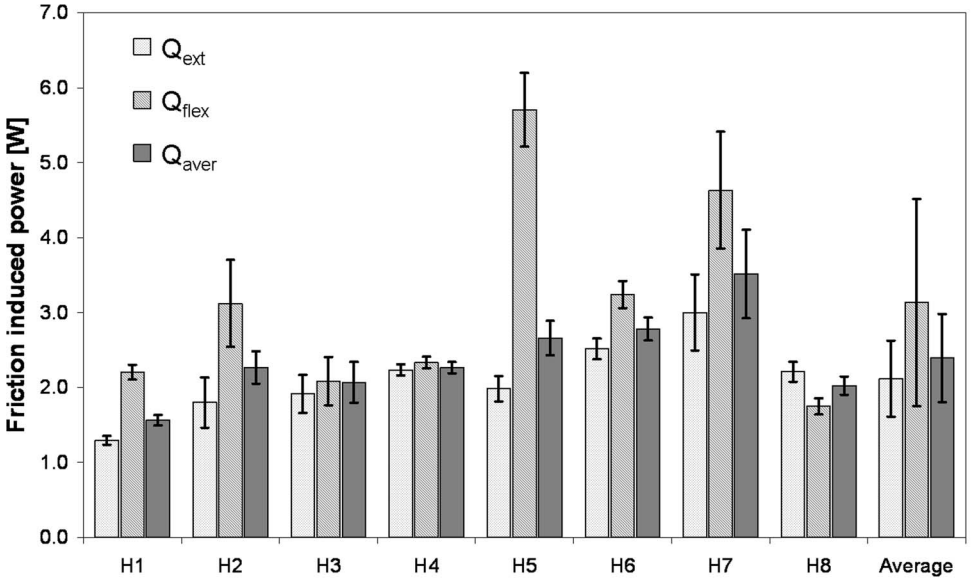

Figure 5. Average friction-induced power Q during flexion and extension phases and whole walking cycle. Q_{ext} = Q during extension phase; Q_{flex} = Q during flexion phase; Q_{aver} = Q during whole step; Individual values of subjects H1 to H8 and averages (right columns).
doi:10.1371/journal.pone.0078373.g005

Figure 3A contains individual numerical averages of the 8 subjects. For $F_{res1}|F_{res2}$ peak values of 248|233% BW at 31|57% of the gait cycle were determined. However, these peak forces varied widely inter-individually. F_{res1} ranged from 210% BW (subject H3) to 301% BW (H8), and F_{res2} from 218% BW (H3) to 287% BW (H8). In 6 subjects F_{res1} was higher than F_{res2}, but in H2 and H3 F_{res1} was lower than F_{res2}. The peak forces during the repeated trials of the same subject had standard deviations in the ranges of 7–14% BW (F_{res1}) and 5–14% BW (F_{res2}).

Friction moments

Figure 2B shows the time courses of M_{res} and its components. M_{res} increased from heel strike (HS) to CHS and reached values of $M_{res1}|M_{res2}$ = 0.16|0.21% BWm. The maximum M_{max} = 0.22% BWm acted slightly later than the force maximum F_{res2}. M_{res} climbed to a second, smaller peak of 0.19% BWm, which acted 15% of the cycle time after CHS, but before toe off of the ipsilateral leg (TO). During the intermediate minimum between CHS and TO, the joint rotation changed from extension to flexion. From HS to CHS, M_{res} was predominantly determined by component M_x, which acts in the sagittal plane of movement. After that and until the end of the stance phase the absolute values of M_y in the frontal plane exceeded those of M_x.

The patterns and magnitudes of M_x were relatively uniform for all 8 subjects (Figure 4A). On average the maximum of M_y had nearly the same magnitude as that of M_x (Figure 4B). The individual maxima of M_y (second peak value in subject H7) acted at very similar times. However, the variation of the individual maxima was much larger compared to M_x. Especially during the first half of the stance phase the time courses of M_y individually varied greatly. On average the peak value of the moment M_z was about ¼ of that of M_x or M_y (Figure 4C). The individual time courses of M_z were similar, but the magnitudes varied considerably.

Figure 3B shows the averages and ranges of the peak values of M_{res} at the times of $F_{res1}|F_{res2}$. $M_{res1}|M_{res2}$ individually varied extremely with inter-trial standard deviations of 0.01 to 0.03% BW for both peak moments M_{res1} and M_{res2}. M_{res1} ranged from 0.12% BWm (H2) to 0.23% BWm (H1), while M_{res2} lay between 0.15% BWm (H3) and 0.29% BWm (H7). In 7 subjects M_{res} increased between the times of F_{res1} and F_{res2} (Figure 4D), with peak values of M_{max} between 0.2% BWm (H8) and 0.32% BWm (H4); it decreased only in H3, but increased again after the time of F_{res2}. In 5 subjects M_{max} occurred with a time delay after F_{res2} between 6% (H4) and 16% (H2) of the gait cycle; in 1 patient M_{max} occurred 2% before F_{res2} (H7), and in 2 subjects, no time delay was observed (H5 and H8). The individual inter-trial standard deviations of M_{max} lay between 0.01 and 0.03% BWm.

Friction coefficients

At HS μ was the lowest with an average value of μ = 0.02 (Figure 2C) and then increased nearly linearly. The values at the times of $F_{res1}|F_{res2}$ were $\mu_1|\mu_2$ = 0.04|0.06. After the instant when the joint rotation changed from extension to flexion, μ rose dramatically and reached its maximum μ_{max} = 0.14, shortly before TO.

The individual numerical values of μ at the instants of $F_{res1}|F_{res2}$ varied by a factor of 2 (Figure 3B); μ_1 had values between 0.03 (lowest in H2, H4, H8) and 0.06 (highest in H3); μ_2 varied between 0.04 (H3, H8) and 0.08 (H7). The maxima μ_{max}, which occurred shortly before TO, varied more, with values between 0.09 (H8) and 0.23 (H2).

The average patterns of the coefficients μ_x, μ_y, μ_z, calculated by the two-dimensional approaches, changed throughout the whole gait cycle (Figure 2C). μ_x in the main plane of movement corresponded well to μ (3D) throughout most of the loading cycle. However, shortly before and after joint rotation changed from extension to flexion, μ_x fell to zero. During the flexion phase, especially at its end, μ_x also deviated from μ. A temporary decline similar to μ_x was also observed for μ_z in the plane of femur rotation, when joint movement changed from extension to flexion. At the same time μ_y in the abduction-adduction plane reached a maximum.

Friction-induced power

With Q_{flex} = 5.0 W, the highest friction-induced power was observed in subjects H5 and H7 during the flexion phase (Figure 5),

although F_{res} and M_{res} were very small (Figure 2A) during most of this period. In 7 of the 8 subjects, Q_{flex} was higher than Q_{ext}, which was mainly due to the higher values of μ and v during flexion (equation 11a, b). The individual differences between Q_{flex} and Q_{ext} varied considerably (Figure 5). The greatest difference was calculated for H5, in which Q_{Flex} was 2.9 times higher than Q_{ext}. The smallest difference was 4%, observed in H4. In H8, Q_{flex} was 21% lower than Q_{ext}. The inter-individual average power throughout the whole cycle was $Q_{aver} = 2.3$ W, with a range between 1.4 W (H1) and 3.8 W (H7). The average sliding speed during flexion was 2.2 times higher than during extension (Table 1), with individual values between 1.5 (H8) and 4.5 (H5).

Discussion

This study reports for the first time on the assessment of *in vivo* friction in artificial hip joints during walking. The *in vivo* measured friction moment, at 3 month post-operative, increased during every gait cycle and as a consequence the coefficient of friction.

Forces and friction moments

Different *in vitro* test conditions were applied by others when investigating friction in hip joint prostheses. Several studies investigated friction by moving the joint in one plane like a pendulum [18,19,29,30], simulating flexion/extension, and neglected movement around the other 2 axes. Our results show that these test conditions may be much too simplified. In reality the abduction-adduction moment M_y rises to nearly the same peak value (0.18% BWm) as the flexion-extension moment M_x (0.2% BWm). Additionally, the joint contact force is not sinusoidal. It may affect the re-formation of a lubricating film during the swing phase when applying a sinus-load.

The resultant moment M_{res} shows a different time-course than the resultant force F_{res} (Figure 2A, B). Although the second force maximum is slightly lower than the first one, the moment is much higher at the instant of the second force peak. This is because friction continuously increases during the extension phase of walking (Figure 2C). The additional peak in the moment curve, shortly before TO, is caused by the sharp increase of the moments M_x and M_z when the hip begins to flex (see below). This finding stands in contrast to *in vitro* findings [18,30], which are based on movements in only one plane. In these studies, the moment showed a plateau phase.

Micro-separation during the swing phase, as reported by others [31,32], can alter the lubrication conditions in the joint. This effect was never observed in our subjects, investigated now and in the past. Otherwise fast changes in the directions of F_{res} or one of its components would have been observed.

Coefficient of friction

The coefficient μ increases by 46% from HS to the instant when the joint starts to flex (Figure 2C). Directly after the change of joint movement from extension to flexion, μ rose sharply in all subjects and reached its maximum at about TO, when the resultant force has markedly been fallen already. This effect has not been described previously in such detail.

It must be assumed that the synovia is squeezed out by the high forces during the extension. *In vitro* studies reported that μ increases when the sliding properties change from lubricated to dry [17,21,22,35]. Furthermore numerical studies with hard/hard pairings have shown that the thickness of the fluid film changes in relation to the joint loading during the gait cycle [30,34]. It was shown that the fluid film thickness decreases at the end of the swing phase, and therefore μ and wear rise, if the swing phase load is increased [30]. A higher swing phase load prevents or restrains the re-formation of the lubrication film, required for good lubrication during the subsequent stance phase. If this explanation also holds true for the investigated ceramic/polyethylene combination of head/cup, a higher swing phase load would let μ decrease less sharply after TO and thus raise the level at which μ starts at the next HS.

Moreover, the strong increase of μ when the joint starts to flex could possibly be caused by a breakdown of the fluid film at the temporary stop of the relative joint movement, similar to the *in vitro* observation during the first step after a rest [33].

Another factor influencing the time pattern of μ may be a changing size of the load bearing area between head and cup, perpendicular to the resultant force vector. This could be especially true if μ were dependent on the pressure magnitude. Both factors could not be investigated in this study.

In contrast to previous *in vitro* studies, the *in vivo* coefficient of friction was now determined for the 3D case. The obtained pattern of μ differs from the pattern of μ_x in the main movement plane of the femur. Both coefficients are nearly identical from HS to CHS and deviate by no more than 5%. However, during the flexion phase, the difference between both coefficients increased up to 9% at TO.

Studies with a simple pendulum test determined values of μ_x between 0.04 and 0.09 for a lubricated regime [18,36,37]. This compares well with our finding of $\mu_1 = 0.04$ and $\mu_2 = 0.06$ during the extension phase. However, $\mu_{max} = 0.14$ at the instant of toe off was much higher in our study.

The peak values of F_{res} individually varied by 39%, but the peak values of μ differed by 246% (Figure 3C). The variance of μ is most likely due to individually different lubrication properties of the synovia fluid.

Friction-induced power

The friction-induced temperature rise in ceramic/PE implants has been measured *in vivo* previously [10]. An estimated average friction-induced power of 0.79 W during walking was reported, which is much less than the average of 2.3 W determined in the current study. It may be that heat convection by the blood flow has been underestimated in the previous study. Other reasons for this discrepancy may be differences between the subjects investigated, and the small sizes of both cohorts. This assumption is supported by another result of the cited study, namely that the temperature increase, measured after 1 hour of walking, individually varied by a factor of nearly 3 after the body weight of all subjects had been standardized. A similarly large factor of 2.7 was observed for the friction-induced power Q_{aver}, which decreased to 2.3 after normalizing the body weight.

The large individual differences of Q_{aver} are most likely caused by varying synovia properties, as already indicated by the variations of μ. Additionally, different running-in effects of the gliding partners may affect the friction-induced power. This running-in effect and the expected decrease of μ and Q_{aver} with increased postoperative time will be investigated in a future study.

In conclusion it was shown: The friction moment in the hip joint mainly occurred in the frontal and sagittal plane during walking. The resultant coefficient of friction increased nearly linearly during extension and increased drastically in the beginning of flexion with the maximum value approximately the ipsilateral toe off. This suggests that the synovia is squeezed out of the intra-articular joint space. Furthermore, the peak values of the coefficient of friction were always determined during the flexion phase. This indicates that the lubrication regime certainly changed into a dry phase at every step.

Limitations of the study

There are some limitations to this study: the number of investigated subjects was small; they were younger than the majority of hip-replacement patients; and only one implant type was investigated at only one speed of walking and one time after implantation. However, the large individual variations of friction coefficient and generated power, as well as the changes of the friction coefficient throughout the gait cycle will probably not be much influenced qualitatively by age or materials. The effects of walking speed and postoperative time is currently investigated an additional study.

Acknowledgments

The authors gratefully acknowledge the voluntary collaboration of all subjects.

Author Contributions

Conceived and designed the experiments: PD GB. Performed the experiments: PD JD. Analyzed the data: PD RA. Contributed reagents/materials/analysis tools: PD AB FG AH AB. Wrote the paper: PD GB.

References

1. CJRR (2013) CJRR annual report: Hip and knee replacements in Canada. Canadian Institute for Health Information.
2. Havelin LI, Fenstad AM, Salomonsson R, Mehnert F, Furnes O, et al. (2009) The Nordic Arthroplasty Register Association: a unique collaboration between 3 national hip arthroplasty registries with 280,201 THRs. Acta orthopaedica 80: 393–401. doi:10.3109/17453670903039544.
3. AOA (2007) Australian Orthopaedic Association National Joint Replacement Registry. Annual Report 2007.
4. Huch K, Müller KAC, Stürmer T, Brenner H, Puhl W, et al. (2005) Sports activities 5 years after total knee or hip arthroplasty: the Ulm Osteoarthritis Study. Annals of the Rheumatic Diseases 64: 1715–1720. doi:10.1136/ard.2004.033266.
5. Chatterji U, Ashworth MJ, Lewis PL, Dobson PJ (2004) Effect of total hip arthroplasty on recreational and sporting activity. ANZ journal of surgery 74: 446–449.
6. Flugsrud GB, Nordsletten L, Espehaug B, Havelin LI, Meyer HE (2007) The effect of middle-age body weight and physical activity on the risk of early revision hip arthroplasty. Acta Orthopaedica 78: 99–107. doi:10.1080/17453670610013493.
7. Malchau H, Herberts P, Söderman P, Odén A (2000) Prognosis of Total Hip Replacement. The swedish national hip arthroplasty registry.
8. Bergmann G, Deuretzbacher G, Heller M, Graichen F, Rohlmann A, et al. (2001) Hip contact forces and gait patterns from routine activities. Journal of biomechanics 34: 859–871.
9. Bergmann G, Graichen F, Rohlmann A (1993) Hip joint loading during walking and running, measured in two patients. Journal of biomechanics 26: 969–990.
10. Bergmann G, Graichen F, Rohlmann A, Verdonschot N, Van Lenthe GH (2001) Frictional heating of total hip implants. Part 2: finite element study. Journal of biomechanics 34: 429–435.
11. Bergmann G, Graichen F, Rohlmann A, Verdonschot N, Van Lenthe GH (2001) Frictional heating of total hip implants. Part 2: finite element study. Journal of biomechanics 34: 429–435.
12. Li S, Chien S, Branemark P-I (1999) Heat shock-induced necrosis and apoptosis in osteoblasts. Journal of orthopaedic research 17: 891–899. doi:10.1002/jor.1100170614.
13. Hall RM, Unsworth A (1997) Review Friction in hip prostheses. Biomaterials 18: 1017–1026.
14. Mattei L, Di Puccio F, Piccigallo B, Ciulli E (2011) Lubrication and wear modelling of artificial hip joints: A review. Tribology International 44: 532–549. doi:10.1016/j.triboint.2010.06.010.
15. Xiong D, Ge S (2001) Friction and wear properties of UHMWPE/Al2O3 ceramic under different lubricating conditions. 250: 242–245.
16. Bergmann G, Graichen F, Rohlmann A, Bender A, Heinlein B, et al. (2010) Realistic loads for testing hip implants. Bio-medical materials and engineering 20: 65–75. doi:10.3233/BME-2010-0616.
17. Bishop NE, Hothan A, Morlock MM (2012) High Friction Moments in Large Hard-on-Hard Hip Replacement Bearings in Conditions of Poor Lubrication. Journal of Orthopaedic Research: 1–7. doi:10.1002/jor.22255.
18. Brockett C, Williams S, Jin Z, Isaac G, Fisher J (2006) Friction of Total Hip Replacements With Different Bearings and Loading Conditions. Journal of Biomedical Materials Research: 508–515. doi:10.1002/jbmb.
19. Scholes SC, Unsworth A, Goldsmith AAJ (2000) A frictional study of total hip joint replacements. Physics in medicine and biology 45: 3721–3735.
20. Scholes SC, Unsworth A, Hall RM, Scott R (2000) The effects of material combination and lubricant on the friction of total hip prostheses. Wear 241: 209–213. doi:10.1016/S0043-1648(00)00377-X.
21. Unsworth A (1978) The effects of lubrication in hip joint prostheses. Physics in medicine and biology 23: 253–268.
22. Scholes SC, Unsworth A (2000) Comparison of friction and lubrication of different hip prostheses. Proceedings of the Institution of Mechanical Engineers Part H Journal of engineering in medicine 214: 49–57.
23. Damm P, Graichen F, Rohlmann, Bender A, Bergmann G (2010) Total hip joint prosthesis for in vivo measurement of forces and moments. Medical Engineering & Physics 32: 95–100.
24. Graichen F, Arnold R, Rohlmann, Bergmann G (2007) Implantable 9-channel telemetry system for in vivo load measurements with orthopedic implants. IEEE transactions on bio-medical engineering 54: 253–261. doi:10.1109/TBME.2006.886857.
25. Graichen F, Bergmann G, Rohlmann (1994) Telemetric transmission system for in vivo measurement of the stress load of an internal spinal fixator. Biomedizinische Technik Biomedical engineering 39: 251–258.
26. Bergmann G, Graichen F, Rohlmann A, Westerhoff P, Heinlein B, et al. (2008) Design and calibration of load sensing orthopaedic implants. Journal of biomechanical engineering 130: 021009. doi:10.1115/1.2898831.
27. Wu G, Siegler S, Allard P, Kirtley C, Leardini A, et al. (2002) ISB recommendation on definitions of joint coordinate system of various joints for the reporting of human motion – part I: ankle, hip, and spine. Journal of Biomechanics 35: 543–548. doi:10.1016/j.pathophys.2011.08.001.
28. Bender A, Bergmann G (2011) Determination of Typical Patterns from Strongly Varying Signals. Computer Methods in Biomechanics and Biomedical Engineering iFirst: 1–9. doi:10.1080/10255842.2011.560841.
29. Saikko V (1992) A simulator study of friction in total replacement hip joints. Proceedings of the Institution of Mechanical Engineers Part H Journal of engineering in medicine 206: 201–211.
30. Williams S, Jalali-Vahid D, Brockett C, Jin Z, Stone MH, et al. (2006) Effect of swing phase load on metal-on-metal hip lubrication, friction and wear. Journal of biomechanics 39: 2274–2281. doi:10.1016/j.jbiomech.2005.07.011.
31. Blumenfeld TJ, Glaser DA, Bargar WL, Langston GD, Mahfouz MR, et al. (2011) In vivo assessment of total hip femoral head seperation from the acetabular cup during 4 common daily activities. Orthopedics 34: e127–e132. doi:10.3928/014774477-20110427-06.
32. Dennis D, Komistek RD, Northcut EJ, Ochoa J, Ritchie A (2001) In vivo determination of hip joint separation and the forces generated due to impact loading conditions. Journal of biomechanics 34: 623–629.
33. Morlock M, Nassutt R, Wimmer M, Schneider E (2000) Influence of Resting Periods on Friction in Artificial Hip Joint Articulations. Bone: 6–16.
34. Meyer DM, Tichy JA (2003) 3-D Model of a Total Hip Replacement In Vivo Providing Hydrodynamic Pressure and Film Thickness for Walking and Bicycling. Journal of Biomechanical Engineering 125: 777. doi:10.1115/1.1631585.
35. Hall RM, Unsworth A, Wroblewski BM, Siney P, Powell NJ (1997) The friction of explanted hip prostheses. British journal of rheumatology 36: 20–26.
36. Hall RM, Unsworth A (1997) Friction in hip prostheses. Biomaterials 18: 1017–1026.
37. Jin Z, Stone M, Ingham E, Fisher J (2006) (v) Biotribology. Current Orthopaedics 20: 32–40. doi:10.1016/j.cuor.2005.09.005.